

# Cosmic-ray antiproton excess from annihilating tensor dark matter.

H. Hernández-Arellano\* and M. Napsuciale†

*Departamento de Física, Universidad de Guanajuato, Lomas del Bosque 103,  
Fraccionamiento Lomas del Campestre, 37150, León, Guanajuato, México.*

S. Rodríguez‡

*Facultad de Ciencias Físico-Matemáticas, Universidad Autónoma de Coahuila,  
Edificio A, Unidad Camporredondo, 25000, Saltillo, Coahuila, México.*

In this work we show that the excess of antiprotons in the range  $E_K = 10 - 20 \text{ GeV}$  reported by several groups in the analysis of the AMS-02 Collaboration data, can be explained by the production of antiprotons in the annihilation of dark matter with a  $(1, 0) \oplus (0, 1)$  space-time structure (tensor dark matter). First, we calculate the proton and antiproton flux from conventional mechanisms and fit our results to the AMS-02 data, confirming the antiproton excess. Then we calculate the antiproton production in the annihilation of tensor dark matter. For the window  $M \in [62.470, 62.505] \text{ GeV}$  to which the measured relic density, XENON1T results and the gamma ray excess from the galactic center constrain the values of the tensor dark matter mass, we find sizable contributions of antiprotons in the excess region from the annihilation into  $\bar{b}b$  and smaller contributions from the  $\bar{c}c$  channel. We fit our results to the AMS-02 data, finding an improvement of the fit for these values of  $M$ .

## I. INTRODUCTION

One of the major challenges in particle physics, astrophysics and cosmology is the elucidation of the nature of dark matter. There is compelling evidence for the existence of dark matter from galaxy rotation curves and observables required to fit the precision measurements of the cosmic microwave background, among them, the dark matter relic density (a recent review on the subject can be found in [1]). For decades, a great effort has been put in the measurement of observables that help us to constrain the values of the mass and possible couplings to the standard model fields of this type of matter that conforms around 26% of the energy budget in the universe. Several experiments have been designed aiming to detect signals of non-gravitational dark matter interactions in direct, indirect and collider searches. In particular, instruments such as PAMELA and AMS-02 have measured with good precision the antimatter cosmic-ray spectrum [2–5], which may include antimatter produced in the annihilation of dark matter.

In the past decade, several reports indicate the existence of an excess of antiprotons in the  $\sim 10 - 20 \text{ GeV}$  region of the AMS-02 Collaboration data, and many studies have identified a consistency with an additional contribution from annihilating dark matter [6–14] (see however alternative explanations to the excess regarding secondary cosmic-rays and systematic errors in [15, 16]). It is interesting to note that most of these studies scan independently the values of  $\langle\sigma v_r\rangle$  for the annihilation of dark matter into standard model channels producing antiprotons in subsequent processes, and the dark matter mass,  $M$ , to conclude that it is possible to explain this excess if dark matter has a mass  $M \sim 60 \text{ GeV}$  and an annihilation cross-section into standard model particles of the order of the thermal relic cross section ( $\langle\sigma v_r\rangle \sim 10^{-26} \text{ cm}^3/\text{seg}$ ).

On the other side, an excess in the gamma ray signal from the galactic center has been claimed by several groups [17–23] and the possibility that this excess be explained by the annihilation of dark matter has been explored scanning independently the values of the annihilation cross section  $\langle\sigma v_r\rangle$  for different standard model channels producing gamma rays in the final state, and the dark matter mass, concluding that similar values can explain the gamma ray excess.

Recently, we proposed an unconventional  $(1, 0) \oplus (0, 1)$  space-time structure for dark matter [24]. In this formalism, dark matter fields are described by a six-component Dirac-like spinor transforming in the  $(1, 0) \oplus (0, 1)$  representation of the Homogenous Lorentz Group (HLG). This theory uses the covariant basis of  $6 \times 6$  matrices for this space constructed in [25] and it is based on simultaneous parity and Poincarè projectors, which yields an equation of motion which differs from the one proposed by Weinberg for these fields long ago [26]. The new equation of motion can be derived from a suitable Lagrangian and the theory turns out to have second class constraints, which can be solved using conventional Dirac's method which replaces Poisson brackets by Dirac brackets. The details of the classical theory and its canonical quantization were given in [27], where it is shown that Fock states can be constructed and

---

\* email:h.hernandezarellano@ugto.mx, corresponding author

† email:mauro@fisica.ugto.mx

‡ email:simonrodriguez@uadec.edu.mx

the formalism do not suffer from the well known tachyonic solutions of the Weinberg equation (for a comprehensive list of references on this point see e.g. [28] and for a recent proposal to use high spin fields in the Weinberg's theory for dark matter applications in an effective field theory approach in spite of these complications we refer to [29]).

The field transforming in the  $(1, 0) \oplus (0, 1)$  representation space was named *spin-one matter field* in [27] because it is the direct generalization of the  $(1/2, 0) \oplus (0, 1/2)$  (Dirac) representation under which transform matter fields in the standard model. Conventionally, fields transforming in the  $(1, 0) \oplus (0, 1)$  are described by a tensor with two antisymmetric Lorentz indices and are named tensor fields. We stick to the historical name here and call the proposed dark matter field transforming in this representation *tensor dark matter field* (TDM).

There is a chirality operator ( $\chi$ ) in the theory and TDM fields can be splitted into left and right fields but, unlike the Dirac theory, the kinetic term of TDM fields couple them, thus charged tensor dark matter cannot have chiral gauge interactions, although vector interactions are allowed [27]. The effective theory for interactions with standard model fields in a hidden scenario yields three dimension-four operators. Two of them couple TDM with the Higgs boson, among which one of them respects parity and the other one violates this symmetry. The corresponding dimensionless couplings are denoted as  $g_s$  and  $g_p$  respectively. The third operator couples the  $Z^0$  and  $\gamma$  to the higher multipoles of TDM, and the corresponding coupling is denoted as  $g_t$ .

In a first panoramic study of the constraints from available data, it was shown that the measured relic density and invisible  $Z$  width constrain the TDM mass to  $M > 43 \text{ GeV}$ . Also, XENON1T upper bounds for the spin independent dark matter-nucleon cross section [30], constrain the spin portal coupling to  $g_t < 10^{-4}$  for TDM masses of the order of hundreds of GeV and sensible values,  $g_s \leq 10^{-1}$ , are compatible with these upper bounds [24]. Similarly, indirect detection upper bounds to the annihilation of dark matter into  $\bar{b}b$ ,  $\tau^+\tau^-$  and  $\mu^+\mu^-$  are satisfied for a wide range of values of  $M$ .

Recently, we studied the possibility that the excess in the gamma-ray spectrum from our galactic center be explained by the annihilation of tensor dark matter [31]. In a comprehensive study of the possible mechanisms, we found that the gamma ray excess can be accounted for by the annihilation of TDM only if  $M \in [62.470, 62.505] \text{ GeV}$ . For a given  $M$  in this window, the measured relic density,  $\Omega_{DM}^{exp} h^2 = 0.1186 \pm 0.0020$  [32, 33], yields the corresponding value  $g_s(M)$  (see Fig.10 of [31]), which takes values in the range  $g_s(M) \in [0.98, 1.01] \times 10^{-3}$ . These values of the TDM mass are at the Higgs resonance for non-relativistic dark matter, thus we refined our previous calculations to focus on the resonance region and to account for the resonant effects in the calculation of the relic density, finding these values compatible with its experimental value, the XENON1T upper bounds on the dark matter-nucleon spin independent cross section, the upper bounds to the annihilation of dark matter into  $\bar{b}b$ ,  $\tau^+\tau^-$  and  $\mu^+\mu^-$  from indirect detection experiments [34–37] and also with the upper bounds for the annihilation into  $\gamma\gamma$  from the FermiLAT [38] and HESS [39] collaborations.

For the values of  $M \in [62.470, 62.505] \text{ GeV}$  and the correlated values  $g_s(M) \in [0.98, 1.01] \times 10^{-3}$ , we get  $\langle \sigma v_r \rangle$  of the order of the thermal cross section for the annihilation into a fermion pair. Fermion pairs (quark and leptons) produced in the annihilation of TDM hadronize (in the case of quark jets) or decay into hadronic states (in the case of leptons) producing other particles, including antiprotons. This signal could be sizable enough to be detected on Earth by any of the current anti-matter measuring experiments, including PAMELA and AMS-02. Annihilation into  $\bar{b}b$  is expected to play a major role in the antiproton production, but there could also be important contributions from the  $\bar{c}c$  and  $\tau^+\tau^-$  channels.

In this paper we explore the possibility that the antiproton excess be explained by antiproton production in the annihilation of TDM. Our work is organized as follows. In the next section we calculate the antiproton and proton cosmic-ray spectrum in the galaxy using standard methods, reproduce results in the literature for the production of antiprotons from standard sources and confirm an excess of antiprotons with  $E_K$  around  $10 - 20 \text{ GeV}$ . In section III, we include the contribution from TDM annihilation into fermions. We fit the obtained flux to AMS-02 data and compare the corresponding  $\chi^2$  to the analogous results without TDM contributions to check if there is a clear preference for TDM annihilation contributions. Our conclusions are given in Section IV.

## II. ANTIPROTON EXCESS IN THE COSMIC-RAY SPECTRUM

The need to collect data on the existing antimatter in the universe that help us in the uncovering of the mystery of the observed baryon asymmetry, prompted the search and eventual detection of cosmic ray (CR) antiprotons during the 1970's [40, 41]. Following several measurements and model proposals for the generation of antiparticles in the Galaxy, it was concluded that CR antiprotons are produced after interactions between high-energy nuclei (cosmic ray primaries, i.e. those accelerated by remnants of supernovae) and matter (mostly hydrogen and helium [42]) within the interstellar medium (ISM), thus they are called secondary antiprotons. Antiprotons could be produced directly (primary antiprotons), either in regions consisting of antimatter (not yet observed) [43], or it could be a product of evaporation of primordial black holes [44]. However, the spectrum of antiprotons observed at Earth is in agreement

with mostly that of secondary origin [45]. The particular kinematics of their production makes their energy spectrum to have a maximum near  $2\text{ GeV}$  and then decrease at energies around tenths of  $\text{GeV}$  in a steeper form than that of protons [46]. This results in a steep decrease in the antiproton-to-proton ratio at these energies. The antiproton flux is thus determined by CR propagation and interaction of nuclei with interstellar gas, processes which suffer from large uncertainties that must be treated carefully in order to predict the flux with high precision.

The first source of systematic uncertainty comes from the CR propagation which involves several complicated processes such as diffusion, convection, re-acceleration and loss of energy. The parameters of choice to model such effects must account for secondary-to-primary nuclei ratios, among which are Boron-to-Carbon (B/C) and other nuclei [47]. A second source of uncertainty is the effect of solar modulation on the CR spectra [48]. When CR enter the Solar System, the solar magnetic field modifies their spectra. This mainly acts on the low energy part of the spectrum, but it is difficult to estimate it with precision since it requires the modeling of the solar wind and its effects, which change through time. For an overview of the effects of solar modulation of the cosmic rays entering the heliosphere, see Ref. [49]. In addition to these, another important source of uncertainties in CR antiproton production is the limited characterization of the cross sections for the production, annihilation and scattering of these particles. In this section we will take this into account and will make use of the parameter choice in the first model in Ref. [12] which yields the best fit to data, to evaluate the proton and antiproton flux from cosmic rays.

### A. Modeling the antiproton and proton cosmic-ray spectrum in the galaxy

We make use of the tool GALPROP [50–52], which takes care of solving the transport equation to yield the local flux of the primary and secondary cosmic ray species. Adopting the first model in Table I of [12], we use the input parameters listed in Table I.

Parameter	Value
$\delta$	0.40
$z_L$ (kpc)	5.6
$D_0$ ( $\text{cm}^2\text{s}^{-1}$ )	$4.85 \times 10^{28}$
$v_A$ (km/s)	24.0
$\alpha_1$	1.88
$dv_c/d z $ (km/s/kpc)	1.0
$\alpha_2$	2.38
$R_{br}$ (GV)	11.7

TABLE I: Cosmic-ray injection and propagation model parameters used, adopted from Ref. [12].

The diffusion coefficient is defined by

$$D_{xx}(R) = \beta D_0 (R/4\text{ GV})^\delta, \quad (1)$$

where  $\delta$  is the diffusion index and  $\beta \equiv v/c$ . The details of this choice of parameters and the process of CR injection, diffusion, convection and reacceleration can be found in Ref. [12].

A study of the antiproton production cross section was done in Ref. [53], where it was found that different procedures led to equivalent results, resulting in an uncertainty of 10-20%. In order to account for this uncertainty, we employ the same approach as formulated in [54], where we multiply the antiproton flux prior solar modulation by an scaling factor in the form of an energy-dependent function, defined by

$$N_{CS}(k_{ISM}) = a + b \left[ \ln \left( \frac{k_{ISM}}{\text{GeV}} \right) \right] + c \left[ \ln \left( \frac{k_{ISM}}{\text{GeV}} \right) \right]^2 + d \left[ \ln \left( \frac{k_{ISM}}{\text{GeV}} \right) \right]^3, \quad (2)$$

where  $k_{ISM}$  is the kinetic energy of the cosmic ray in the interstellar medium, before entering the Solar System. The fourth term of this scaling factor, proportional to  $\left[ \ln \left( \frac{k_{ISM}}{\text{GeV}} \right) \right]^3$ , can be omitted and still reach a adequate fit, as we will show later.

We must also consider the effects of solar modulation. The differential flux at Earth,  $dN^\oplus/dE_{kin}$  in terms of  $k_{ISM}$ , is obtained as [48]

$$\frac{dN^\oplus}{dE_{kin}}(k_{ISM}) = \frac{(k_{ISM} - |Z|e\Phi(R) + m)^2 - m^2}{(k_{ISM} + m)^2 - m^2} \frac{dN^{ISM}}{dk_{ISM}}(k_{ISM}), \quad (3)$$

where  $dN^{ISM}/dk_{ISM}$  is the differential flux prior to the effects of solar modulation,  $E_{kin}$ ,  $|Z|e$  and  $m$  are the kinetic energy, charge and mass of the cosmic ray. To obtain the flux in terms of  $E_{kin}$ , we use the equivalence  $E_{kin} = k_{ISM} - |Z|e\Phi(R)$ . The modulation potential,  $\Phi$ , can be described as a function that depends on time, the rigidity ( $R = \sqrt{k_{ISM}(k_{ISM} + 2m_p)}$ ) and charge of the cosmic ray prior entering the Solar System. We follow the analytic expression constructed in Ref. [55]:

$$\Phi(R, t, q) = \phi_0 \left( \frac{|B_{tot}(t)|}{4 \text{ nT}} \right) + \phi_1 N'(q) H(-qA(t)) \left( \frac{|B_{tot}(t)|}{4 \text{ nT}} \right) \left( \frac{1 + (R/R_0)^2}{\beta(R/R_0)^3} \right) \left( \frac{\alpha(t)}{\pi/2} \right)^4, \quad (4)$$

where  $\beta$  is the velocity,  $R_0 \equiv 0.5$  GV and  $B_{tot}$  is the strength of the heliospheric magnetic field (HMF) at Earth, which has a polarity  $A(t)$ ,  $H$  denotes the Heaviside function and  $\alpha$  is the tilt angle of the heliospheric current sheet.  $N'(q) \neq 1$  when the HMF does not have a well-defined polarity.

We allow  $\phi_0 \in [0.32, 0.38]$  GV and  $\phi_1 \in [0, 16]$  GV in order to stand within the uncertainties for the modulation potential described in Ref. [55]. The values of  $B_{tot}$ ,  $\alpha$  and  $N'(q)H(-qA(t))$  averaged over six-month intervals during the observation period by AMS-02 can be found in Table II of [54]. We take these values to evaluate the potential and the flux for each period and then take the average of the obtained values for the final result.

There is an additional parameter, the local ISM gas density normalization, taken as an energy-independent factor,  $g_{ISM}$ . In total, there are seven free parameters that will be used for the fit:  $\phi_0$ ,  $\phi_1$ ,  $a$ ,  $b$ ,  $c$ ,  $d$  and  $g_{ISM}$ . The flux ratio is defined as follows.

$$R_{\bar{p}/p} = \frac{\Phi_{\bar{p}}}{\Phi_p} = g_{ISM} \frac{dN_{\bar{p}}^{\oplus}}{dE_{kin}} \cdot \quad (5)$$

## B. Results of the fit to the antiproton-proton ratio without dark matter

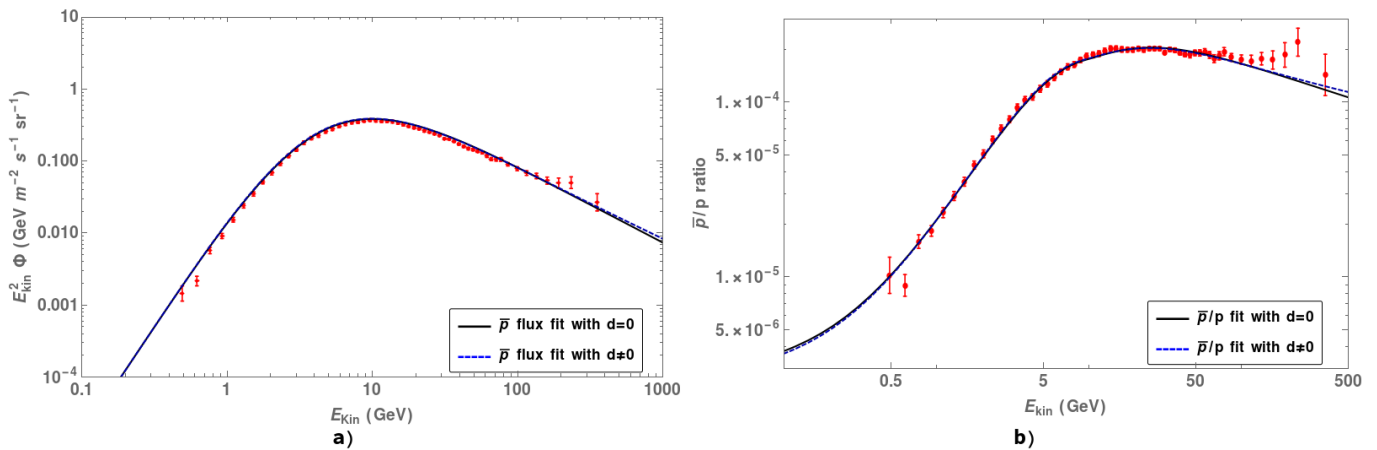


FIG. 1: Best fit to the AMS-02 data on the a) antiproton flux and b) antiproton-to-proton ratio for  $d = 0$  (solid line) and  $d \neq 0$  (dashed line).

The results for the best fit to the AMS-02 antiproton flux and antiproton-to-proton ratio data [56] are shown in Fig. 1. We performed the fit for the two cases,  $d = 0$  (fit 1) and  $d \neq 0$  (fit 2). A summary of the fitting parameters and the corresponding value of  $\chi^2$  for each case is given in Table II. The difference (residual) between the antiproton-to-proton ratio for each fit and the AMS-02 data is shown in Fig. 2. We can see that there is an excess in the residual around  $\sim 10$ -20 GeV and in the higher end of the spectrum.

## III. ANTIPROTON PRODUCTION FROM ANNIHILATING TENSOR DARK MATTER

In the effective field theory for hidden tensor dark matter, the leading interacting terms for the simplest case of a  $U(1)_D$  dark gauge group, turn out to be dimension-four and are given by [24]

$$\mathcal{L}_{int} = \bar{\psi}(g_s \mathbf{1} + ig_p \chi) \psi \phi^\dagger \phi + g_t \bar{\psi} M_{\mu\nu} \psi B^{\mu\nu} + \mathcal{L}_{selfint}, \quad (6)$$

Fit	$\phi_0/GV$	$\phi_1/GV$	a	b	c	d	$g_{ISM}$	$\chi^2$
1	0.3257	16	1.1579	-0.1632	0.0216	0	1.1844	1.0561
2	0.32	16	1.1549	-0.1301	0.0038	0.0023	1.1842	0.9243

TABLE II: Best-fit parameters to the AMS-02 antiproton-to-proton ratio data considering secondary antiprotons produced in the ISM, for  $d = 0$  (fit 1) and  $d \neq 0$  (fit 2).

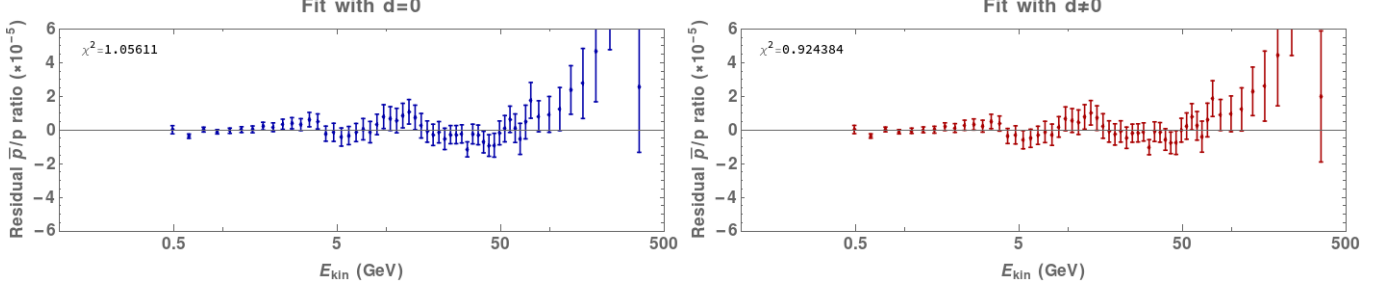


FIG. 2: Antiproton-to-proton ratio residual from the AMS-02 data from Ref. [56].

where  $\psi$  is a six-component "spinor" describing TDM,  $\phi$  is the standard model Higgs doublet and  $g_s$ ,  $g_p$  and  $g_t$  are dimensionless constants. The first two operators yield parity-respecting and parity-violating *Higgs portals* and the third couple the photon and  $Z^0$  to higher multipoles of tensor dark matter and is therefore dubbed *spin portal*. After spontaneous symmetry breaking, this Lagrangian yields

$$\mathcal{L}_{int} = \frac{1}{2} \bar{\psi} (g_s \mathbf{1} + i g_p \chi) \psi (H + v)^2 + g_t C_W \bar{\psi} M_{\mu\nu} \psi F^{\mu\nu} - g_t S_W \bar{\psi} M_{\mu\nu} \psi Z^{\mu\nu}, \quad (7)$$

where  $C_W$ ,  $S_W$ ,  $H$ ,  $v$ , are the cosine and sine of the Weinberg angle, the Higgs field and the Higgs vacuum expectation value, and  $F^{\mu\nu}$ ,  $Z^{\mu\nu}$  stand for the stress tensors of the electromagnetic and  $Z^0$  fields.

Tensor dark matter can annihilate into fermion-anti-fermion through the Higgs portals and the spin portal in Eq. (7). We refer the reader to Ref. [24] for technical details of the calculation of the cross sections for the annihilation of TDM into standard model particles. The cross section for the annihilation into a fermion-anti-fermion pair is [24]

$$\begin{aligned} \langle \sigma v_r \rangle_{\bar{f}f}(s) = & \frac{N_c}{144\pi M^4 \sqrt{s}} \frac{\sqrt{s - 4m_f^2}}{(s - M^2)} \left[ \frac{m_f^2 (s - 4m_f^2) (g_p^2 s (s - 4M^2) + g_s^2 (6M^4 - 4M^2 s + s^2))}{((s - M_H^2)^2 + \Gamma_H^2 M_H^2)} \right. \\ & + \frac{2g_t^2 M_Z^2 S_W^2 s (s - 4M^2) (2M^2 + s) (2(A_f^2 - 2B_f^2) m_f^2 + s(A_f^2 + B_f^2))}{3v^2 ((s - M_Z^2)^2 + \Gamma_Z^2 M_Z^2)^2} \\ & + \frac{32C_W^2 Q_f^2 g_t^2 M_W^2 S_W^2 (s - 4M^2) (2M^2 + s) (2m_f^2 + s)}{3v^2 s} \\ & \left. - \frac{16A_f C_W Q_f g_t^2 M_W M_Z S_W^2 (s - 4M^2) (2M^2 + s) (2m_f^2 + s)}{3v^2 ((s - M_Z^2)^2 + \Gamma_Z^2 M_Z^2)} \right], \quad (8) \end{aligned}$$

where  $N_c = 3$  for quarks and  $N_c = 1$  for leptons,  $m_f$ ,  $Q_f$  correspond to the mass of the fermion and its charge in units of  $e > 0$ , respectively, and

$$A_f = 2T_f^{(3)} - 4Q_f \sin^2 \theta_W, \quad B_f = -2T_f^{(3)}. \quad (9)$$

In the non-relativistic limit, only the parity-conserving Higgs portal contributions survive and the velocity averaged cross section reads

$$\langle \sigma v_r \rangle_{\bar{f}f} = \frac{N_c g_s^2 m_f^2 (M^2 - m_f^2)^{\frac{3}{2}}}{12\pi M^3 [(4M^2 - M_H^2)^2 + M_H^2 \Gamma_H^2]} + \mathcal{O}(v_r^2). \quad (10)$$

Notice that  $\langle\sigma v_\tau\rangle_{\bar{f}f}$  and the TDM mass  $M$  are not independent parameters, thus the predictions are specific to the nature (space-time structure) of TDM. In order to keep consistency with the measured dark matter relic density, upper limits by XENON1T for the spin-independent dark matter-nucleon cross-section, indirect detection limits and the gamma-ray excess at the Milky Way galactic center, we consider in our calculations  $M \in [62.470, 62.505]$  GeV. For a given value of  $M$  the corresponding value of  $g_s(M)$  is fixed by the measured relic density given in Fig. 10 of Ref. [31].

We use the PPC4DMID code [57] to obtain the antiproton flux produced in the hadronization of quarks or the hadronic decay of the  $\tau$  lepton produced in the annihilation of TDM, and its propagation in the ISM. The code uses Monte Carlo simulations in order to find the differential spectra of antiprotons, including electroweak corrections. Although protons are also produced by the same mechanism, its contribution to the overall proton flux is very small and can be neglected. Only the antiproton production is large enough to be relevant in the calculation of the antiproton to proton flux ratio. The contributions of the relevant channels to the antiproton-proton ratio are shown in Fig. 3, where we can see that the  $\bar{b}b$  and  $\bar{c}c$  channels yield an antiproton flux with a maximum in the energy range of the excess in the AMS-02 data and it is dominated by the  $\bar{b}b$  channel.

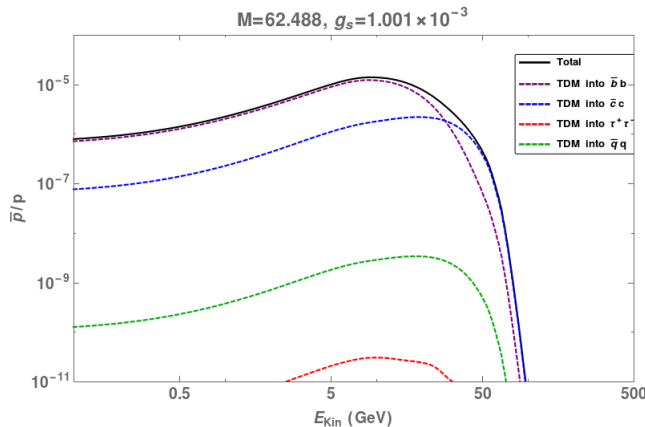


FIG. 3: Antiproton-to-proton flux ratio for antiprotons produced in the annihilation of TDM for  $M = 62.488$  GeV and the correlated coupling  $g_s(M) = 1.001 \times 10^{-3}$ , for the  $\bar{b}b$ ,  $\bar{c}c$ ,  $\tau^+\tau^-$  and light quark channels.

### A. Results of the fit to the antiproton-proton ratio including tensor dark matter contributions

In order to assess the statistical relevance of this contribution we fitted the total flux to the AMS-02 data for both cases,  $d = 0$  and  $d \neq 0$ , for fixed value of the mass  $M$ . Scanning the whole range  $M \in [62.470, 62.505]$  GeV we obtain results shown in Fig. 4 for the  $\chi^2$  of the fit including TDM contributions and compare it to the value for the best fit without TDM contributions obtained in the previous section for  $d = 0$  and  $d \neq 0$ . We can see that the fit improves for all values of  $M \in [62.470, 62.505]$  GeV in both cases. In these plots we also mark with a point the minimal value of  $\chi^2$  for the considered values of  $M$ . These points correspond to the best fit including TDM contributions in each case. The parameters corresponding to these points are given in Table III. In the case  $d = 0$ , the best fit is obtained for  $M = 62.4839$  GeV and the corresponding value of the spin portal coupling compatible with the measured relic density is  $g_s(M) = 1.0053 \times 10^{-3}$ . As to the  $d \neq 0$  case the best fit yields  $M = 62.4877$  GeV and the corresponding coupling is  $g_s(M) = 1.0009 \times 10^{-3}$ .

Fit	$M/GeV$	$\phi_0/GV$	$\phi_1/GV$	<b>a</b>	<b>b</b>	<b>c</b>	<b>d</b>	$g_{ISM}$	$\chi^2$
3	62.4839	0.32	16	1.1216	-0.1599	0.0247	0	1.1371	0.8783
4	62.4877	0.32	16	1.1225	-0.1691	0.0290	-0.00043	1.1310	0.8772

TABLE III: Best-fit parameters to the AMS-02 antiproton-to-proton ratio for  $d = 0$  (Fit 3) and  $d \neq 0$  (Fit 4), including antiprotons from TDM annihilation.

The separate signals for the parameters of the best-fit results in Table III are shown in Fig. 5, where data points correspond to the antiproton-proton residual ratio from the AMS-02 data for antiprotons produced in the ISM and the continuous lines correspond to antiprotons produced in the annihilation of TDM. We can see in these plots that

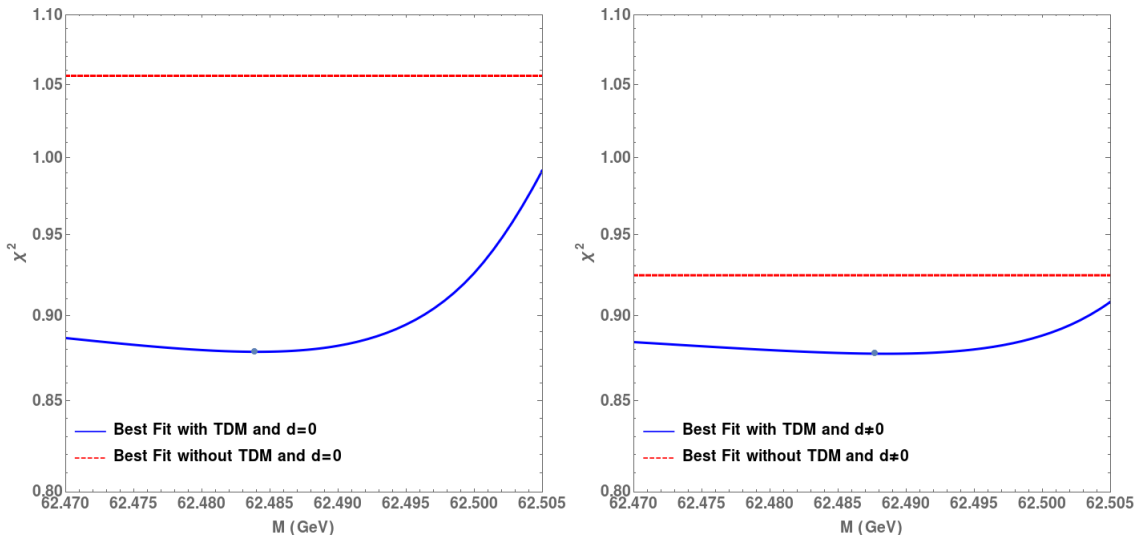


FIG. 4:  $\chi^2$  value as a function of  $M$ , for  $d = 0$  (left) and  $d \neq 0$  (right). The dashed lines are the  $\chi^2$  values without the TDM annihilation contributions in Section II. The points correspond to the minimal value in each case.

TDM contributions account for the antiprotons excess extracted from the AMS-02 data and this result is not sensitive to the value of  $d$ .

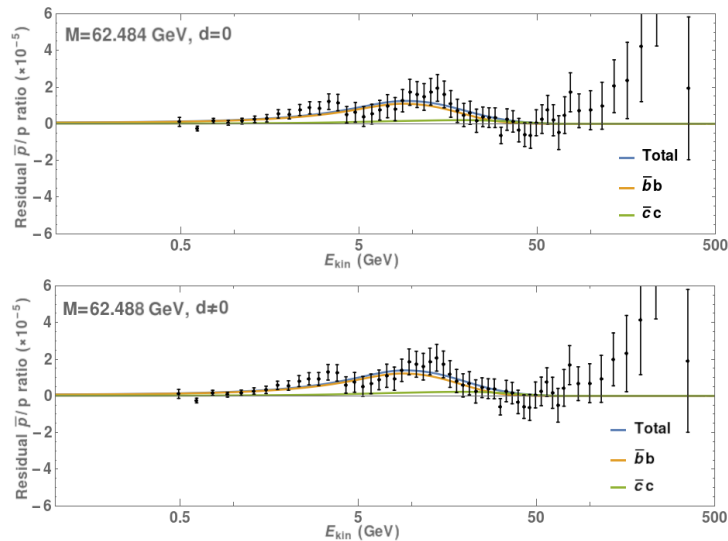


FIG. 5: Antiproton-to-proton ratio pure residual (annihilation contributions not included) from the AMS-02 data [56] for the parameters in the best fit for  $d = 0$  (top) and  $d \neq 0$  (bottom) in Table III. In both cases we also show the contributions from TDM annihilation into  $\bar{b}b$  and  $\bar{c}c$  for the corresponding value of  $M$  in Table III.

#### IV. CONCLUSIONS

In this work we study the production of antiprotons in the annihilation of tensor dark matter and the possibility that it explains the cosmic-ray antiprotons excess with  $E_K$  around  $10 - 20$  GeV in the AMS-02 data claimed by several groups. First we use the GALPROP tool to solve the transport equation in order to evaluate the proton and antiproton flux produced in the interstellar medium. The largest uncertainty ( $10 - 20$  %) in this calculation comes from the estimate of the cross-section for the antiproton production in the ISM. Following [54], we introduce a scaling factor in the antiproton to proton flux ratio to study effects of this uncertainty. The fits are improved by this scaling

factor and our results confirm an excess of antiprotons in the  $\sim 10 - 20$  GeV region of the spectrum.

Then, we use the PPC4DMID code to calculate the flux of antiprotons produced in the hadronization and propagation of quarks or in the hadronic decays of leptons produced in the annihilation of tensor dark matter. The corresponding velocity averaged cross sections depend only on the TDM mass  $M$  and the coupling  $g_s$  of the parity-conserving Higgs portal in the effective theory. The value of the TDM mass is constrained to the narrow windows  $M \in [62.470, 62.505]$  GeV by the measured relic density, the gamma ray excess from the galactic center and the upper bounds for the dark matter-nucleon spin independent cross section measured by XENON and, for a given value of  $M$ , the measured dark matter relic density fixes the value  $g_s(M)$  which takes values in the range  $g_s(M) \in [0.98, 1.01] \times 10^{-3}$ , such that we have actually only one independent parameter. These range of values are also consistent with the upper bounds for the annihilation of dark matter into  $\bar{b}b$ ,  $\tau^+\tau^-$ ,  $\mu^+\mu^-$  and  $\gamma\gamma$  from indirect detection searches in gamma ray physics [31]. We find a sizable antiproton flux from the annihilation of tensor dark matter for these values of  $M$ . The main contribution comes from TDM annihilation into  $\bar{b}b$ , the  $\bar{c}c$  channel contribution being roughly two orders of magnitude smaller and other contributions negligible. This antiproton flux has a maximum for  $E_K$  in the region of the antiproton excess.

In order to assess the statistical significance of antiprotons produced in the annihilation of tensor dark matter we perform fits to the AMS-02 data for the antiproton to proton ratio including these contributions for fixed  $M$ , finding that it improves the fits for the whole range of mass  $M \in [62.470, 62.505]$  GeV. The best fit is obtained for  $M = 62.4877$  GeV and the corresponding coupling for the parity-conserving Higgs portal in the effective theory is fixed by the measured relic density to  $g_s(M) = 1.0009 \times 10^{-3}$ . We conclude that the antiproton excess in the AMS-02 data can be explained by antiprotons produced in the annihilation of tensor dark matter.

## V. ACKNOWLEDGEMENTS

We thank Ilias Cholis for his help in the use of GALPROP to model proton and antiproton flux. H.H.A acknowledges financial support from CONACyT, México to pursue her PhD program.

- 
- [1] T. Lin, PoS **333**, 009 (2019).
  - [2] O. Adriani *et al.*, Science **332**, 69 (2011).
  - [3] M. Aguilar *et al.*, Phys. Rev. Lett. **114**, 171103 (2015).
  - [4] M. Aguilar *et al.*, Phys. Rev. Lett. **115**, 211101 (2015).
  - [5] M. Aguilar *et al.*, Phys. Rev. Lett. **117**, 231102 (2016).
  - [6] T. Bringmann, M. Vollmann, and C. Weniger, Phys. Rev. D **90**, 123001 (2014).
  - [7] M. Cirelli *et al.*, JCAP **12**, 045 (2014).
  - [8] D. Hooper, T. Linden, and P. Mertsch, JCAP **03**, 021 (2015).
  - [9] M.-Y. Cui, Q. Yuan, Y.-L. S. Tsai, and Y.-Z. Fan, Phys. Rev. Lett. **118**, 191101 (2017).
  - [10] A. Cuoco, J. Heisig, M. Korsmeier, and M. Krämer, JCAP **10**, 053 (2017).
  - [11] A. Cuoco, M. Krämer, and M. Korsmeier, Phys. Rev. Lett. **118**, 191102 (2017).
  - [12] I. Cholis, T. Linden, and D. Hooper, Phys. Rev. D **99**, 103026 (2019).
  - [13] S.-J. Lin *et al.*, Phys. Rev. D **96**, 123010 (2017).
  - [14] S. J. Clark, B. Dutta, and L. E. Strigari, Phys. Rev. D **97**, 023003 (2018).
  - [15] J. Heisig, M. Korsmeier, and M. W. Winkler, Phys. Rev. Res. **2**, 043017 (2020).
  - [16] M. Boudaud *et al.*, Phys. Rev. Res. **2**, 023022 (2020).
  - [17] D. Hooper and L. Goodenough, Phys. Lett. **B697**, 412 (2011).
  - [18] A. Boyarsky, D. Malyshev, and O. Ruchayskiy, Phys. Lett. **B705**, 165 (2011).
  - [19] D. Hooper and T. Linden, Phys. Rev. **D84**, 123005 (2011).
  - [20] K. N. Abazajian and M. Kaplinghat, Phys. Rev. **D86**, 083511 (2012), [Erratum: Phys. Rev.D87,129902(2013)].
  - [21] O. Macias and C. Gordon, Phys. Rev. **D89**, 063515 (2014).
  - [22] M. Ackermann *et al.*, Astrophys. J. **840**, 43 (2017).
  - [23] C. Gordon and O. Macias, Phys. Rev. **D88**, 083521 (2013), [Erratum: Phys. Rev.D89,no.4,049901(2014)].
  - [24] H. Hernández-Arellano, M. Napsuciale, and S. Rodríguez, Phys. Rev. D **98**, 015001 (2018).
  - [25] S. Gómez-Ávila and M. Napsuciale, Phys. Rev. D **88**, 096012 (2013).
  - [26] S. Weinberg, Phys. Rev. **133**, B1318 (1964).
  - [27] M. Napsuciale, S. Rodríguez, R. Ferro-Hernández, and S. Gómez-Ávila, Phys. Rev. D **93**, 076003 (2016).
  - [28] J. O. Eeg, Lett. Nuovo Cim. **4S2**, 223 (1972).
  - [29] J. C. Criado, N. Koivunen, M. Raidal, and H. Veermäe, Phys. Rev. D **102**, 125031 (2020).
  - [30] E. Aprile *et al.*, Phys. Rev. Lett. **119**, 181301 (2017).
  - [31] H. Hernández-Arellano, M. Napsuciale, and S. Rodríguez, JHEP **08**, 106 (2020).

- [32] P. A. R. Ade *et al.*, *Astron. Astrophys.* **594**, A13 (2016).
- [33] C. Patrignani *et al.*, *Chin. Phys.* **C40**, 100001 (2016 and 2017 update).
- [34] L. Bergstrom *et al.*, *Phys. Rev. Lett.* **111**, 171101 (2013).
- [35] M. Aguilar *et al.*, *Phys. Rev. Lett.* **110**, 141102 (2013).
- [36] A. Drlica-Wagner *et al.*, *Astrophys. J.* **809**, L4 (2015).
- [37] A. Albert *et al.*, *Astrophys. J.* **834**, 110 (2017).
- [38] M. Ackermann *et al.*, *Phys. Rev.* **D91**, 122002 (2015).
- [39] H. Abdallah *et al.*, *Phys. Rev. Lett.* **120**, 201101 (2018).
- [40] R. L. Golden *et al.*, *Phys. Rev. Lett.* **43**, 1196 (1979).
- [41] E. A. Bogomolov *et al.*, in *International Cosmic Ray Conference, International Cosmic Ray Conference (ICRC, Kyoto, Japan, 1979)*.
- [42] K. M. Ferriere, *Rev. Mod. Phys.* **73**, 1031 (2001).
- [43] C. S. Shen and G. B. Berkey, *Phys. Rev.* **171**, 1344 (1968).
- [44] A. Barrau *et al.*, *Astron. Astrophys.* **388**, 676 (2002).
- [45] A. S. Beach *et al.*, *Phys. Rev. Lett.* **87**, 271101 (2001).
- [46] I. V. Moskalenko, A. W. Strong, J. F. Ormes, and M. S. Potgieter, *Astrophys. J.* **565**, 280 (2002).
- [47] A. W. Strong and I. V. Moskalenko, *The Astrophysical Journal* **509**, 212 (1998).
- [48] L. J. Gleeson and W. I. Axford, *Astrophys. J.*, 154: 1011-26(Dec. 1968). .
- [49] M. Potgieter, *Living Reviews in Solar Physics* **10**, (2013).
- [50] G. team, GALPROP WebRun, <https://galprop.stanford.edu/webrun/>.
- [51] A. Vladimirov *et al.*, *Computer Physics Communications* **182**, 1156 (2011).
- [52] I. Moskalenko, A. Strong, J. Ormes, and S. Mashnik, *Advances in Space Research* **35**, 156 (2005), mars International Reference Atmosphere, *Living With a Star and Fundamental Physics*.
- [53] M. di Mauro, F. Donato, A. Goudelis, and P. D. Serpico, *Phys. Rev. D* **90**, 085017 (2014), [Erratum: *Phys.Rev.D* 98, 049901 (2018)].
- [54] I. Cholis, D. Hooper, and T. Linden, *Phys. Rev. D* **95**, 123007 (2017).
- [55] I. Cholis, D. Hooper, and T. Linden, *Phys. Rev. D* **93**, 043016 (2016).
- [56] M. Aguilar *et al.*, *Phys. Rev. Lett.* **117**, 091103 (2016).
- [57] M. Cirelli *et al.*, *Journal of Cosmology and Astroparticle Physics* **2011**, 051 (2011).